Bromine Enrichment in the Near-Surface Region of Br-Doped NaCl Single Crystals Diagnosed by Rutherford Backscattering Spectrometry

M. Hess,*,§ U. K. Krieger,§ C. Marcolli,§ T. Huthwelker,† M. Ammann,† W. A. Lanford,‡ and Th. Peter§

Institute for Atmospheric and Climate Science, ETH Zurich, 8093 Zurich, Switzerland, Paul Scherrer Institute, 5232 Villigen, PSI, Switzerland, and Physics Department, State University of New York—Albany, Albany, New York 12222

Received: November 9, 2006; In Final Form: March 8, 2007

Bromine released from sea-salt aerosols and seawater ice is known for its high chemical reactivity. Previous studies have suggested that its availability to the gas-phase could be enhanced by segregation processes increasing Br concentration on the aerosol surface as compared to the bulk. However, little is known about the composition within the near-surface region, that is, the outermost ~100 monolayers. We used Rutherford backscattering spectrometry (RBS) to measure Br concentration profiles to a depth of about 750 nm of Br-doped NaCl single crystals to characterize the thermodynamics and kinetics of Br segregation to the near-surface region in moist air. These experiments were carried out on cleavage planes of melt-grown and of annealed solution-grown crystals at room temperature and relative humidities (RH) too low for formation of a stable liquid phase. Segregation of Br was below the detection limit on melt-grown crystals with Br/Cl = 0.01. In the case of annealed solution-grown crystals with Br/Cl = 0.002, average segregations of $(0.24 \pm 0.11) \times 10^{15}$ and $(0.42 \pm 0.12) \times 10^{15}$ Br atoms cm^{-2} were observed at 50% and 65% RH, respectively. No segregation was found at 20% RH. The observed Br segregation can be explained by the formation of an adsorbed liquid layer (depending on crystal surface properties and relative humidity) and preferential, diffusion-limited dissolution of Br into this layer according to the partition coefficient of Br between aqueous and solid NaCl. The thickness of the adsorbed liquid layer, which depends on crystal surface geometry and on relative humidity, can be estimated to range from 4 to at most 59 nm on the basis of measured Br concentrations and partition coefficients. Applying this concept of partitioning to natural sea salt suggests a Br/Cl molar ratio of up to 0.2 in adsorbed surface water of crystallized natural aerosol particles compared to about 0.0015 in seawater. This would have a major impact on heterogeneous reactions on sea-salt particles under dry conditions such as in the freeze-dried Arctic boundary layer.

1. Introduction

Sea salt is the second most abundant particulate matter in the global atmosphere (after dust) and is the dominant aerosol species by mass above the oceans.[1] Heterogeneous reactions of gas-phase constituents on sea-salt aerosols may lead to the generation of highly reactive halogen atoms in the gas phase (e.g., ref 2). Sea-salt aerosols have their highest concentrations in the marine boundary layer; however, they can be transported over large distances and have been observed as much as 900 km inland.[3] Vertical transport of sea salt into the upper troposphere by convection[4] or even into the stratosphere along with volcanic eruptions[5] has been observed. Under some of these conditions, the relative humidity (RH) may fall below the efflorescence point of NaCl (~40% RH[6]), and the originally liquid aerosols may crystallize.

Halogen chemistry is of particular importance in polluted air, since acidification of the air facilitates the halogen release from sea-salt particles via acid ion-exchange reactions (e.g., refs 2, 7, and 8). In remote areas, halogen chemistry can have significant impact on atmospheric chemistry, such as in the depletion events of surface-level ozone at polar sunrise over the Arctic.[9,10] Ozone concentrations can drop from 30 ppbv to almost 0 ppbv within hours, accompanied by an increase of filterable bromine.[9] Such ozone depletion events have been observed not only in the Arctic, but also in the vicinity of saline dry lake beds such as the Dead Sea.[11] An autocatalytic mechanism for the release of reactive bromine from the sea-salt particle has been proposed.[12,13]

Because of its reactivity, the importance of bromine for tropospheric chemistry is disproportionately high. Given the Cl/Br molar ratio in seawater (~660), it is a minor component in sea salt. However, it has been suggested that heterogeneous formation of Br_2 and bromine chemistry in the gas phase in general would be strongly enhanced by a surface enrichment of bromine on aerosol surfaces.[12,13]

The system NaCl−NaBr may form uniform, face centered cubic (fcc) single crystals at any prescribed Br/Cl ratio (i.e., solid solutions whose components are completely miscible at room temperature).[14−16] Since the ion size of Br^- is different from Cl^-, the concentration of Br as the dopant in natural particles is smaller in the crystal than in the surrounding aqueous solution. (Note that we are dealing here with bromide and chloride ions but will suppress the ionic nomenclature as RBS

* To whom correspondence should be addressed. E-mail: maurus.hess@env.ethz.ch.
§ Institute for Atmospheric and Climate Science.
† Paul Scherrer Institute.
‡ State University of New York—Albany.

10.1021/jp0674120 CCC: $37.00
Published on Web 04/27/2007

provides only elemental information). The partitioning of Br between liquid and solid can be expressed as a partition coefficient $p = ([Br]/[Cl])_{crst}/([Br]/[Cl])_{sol}$,[17] and was subject of earlier experimental and theoretical studies.[14,15,17−20] Typically, p was found to range from 0.035 to 0.045 at Br/Cl ratios similar to that in natural sea-salt aerosols. However, Br incorporation into the crystal lattice depends also on the crystal growth rate. In very slowly grown crystals, a lower partition coefficient of $p = 0.014$ was measured,[18,19] which is in close agreement with a calculated value for thermodynamic equilibrium.[21] Furthermore, it was shown that the presence of $MgCl_2$ in the solution decreases the partition coefficient by a factor of about 2.[15,17]

Surface segregation of bromine in Br-doped NaCl single crystals after exposure to moist air has been observed in a previous work.[22] However, only melt-grown crystals with Br/Cl ratios much higher than in natural ocean water were considered, which may lead to results not directly applicable to atmospheric chemistry. Zangmeister et al.[23] found Br surface segregation in NaCl−NaBr crystals after precipitation from aqueous solution and attributed this to the different solubility of NaBr and NaCl in water leading to heterogeneous crystal growth and NaBr-rich domains. These investigations were performed directly on the crystal surface grown from the solution, after drying but without further controlled exposure to humidity.

To our knowledge, no experiments have been performed with solution-grown crystals exposed to humidity. In this study, we investigate the segregation of Br to the near-surface region in Br-doped NaCl single crystals grown from melt and grown from aqueous solution with Br/Cl ratios similar to that of sea-salt. We use Rutherford backscattering spectrometry, because this technique allows measurement of Br concentration profiles into about 750 nm depth of the crystal. On the basis of our results, we suggest a simple model, which allows prediction of the Br concentration on NaCl surfaces under atmospheric conditions applicable to mixed-phase sea-salt aerosols.

2. Experimental Setup

2.1. Rutherford Backscattering Spectrometry (RBS). *Principle.* Rutherford backscattering spectrometry is well described in the literature[24] so only a brief outline is presented here. In RBS, a target is bombarded with a mono-energetic beam of ions (most commonly 2 MeV He^+ ions) and the energies of the ions backscattered from the target are recorded. The recorded spectrum of the number of backscattered ions versus their energy contains information about the elemental target composition versus depth: for a given target composition, the RBS energy spectrum is completely determined by conservation of energy and momentum in two-body collisions, the scattering cross-section (σ), and the rate of energy loss of ions in matter (dE/dx). Hence, RBS spectra can unambiguously be interpreted without use of reference "standard" samples as is commonly the case for other analytical methods. For targets thin enough that the energy loss by ions penetrating the target can be neglected, the energy of the backscattered ion (E) is given by conservation of energy and momentum to be $E = KE_{beam}$, where E_{beam} is the beam energy and K is the kinematic factor that depends only on the scattering angle and the masses of the projectile and target atom. At 180° backscattering, $K = [(M_1 - M_2)/(M_1 + M_2)]^2$ where M_1 is the nuclear mass of the projectile and M_2 is the nuclear mass of the target atom. Hence, the measurement of the backscattered ion energy, E, determines the mass of the target nucleus. In addition, the number of backscattered ions (Y) is given by $dY = \sigma n N\, d\Omega$, where σ is the scattering cross section, n is the number of incident ions, N is the number of target atoms/cm^2, and $d\Omega$ is the solid angle subtended by the detector. For a wide range of projectile ion energies, σ is given by the well-known Rutherford formula, σ_R. For a scattering angle of 180°, $\sigma_R = (Z_1 Z_2 e^2/4E_{beam})^2$, where Z_1 and Z_2 are the atomic numbers of the projectile and target atoms, respectively (note, $e^2 = 1.44 \times 10^{-13}$ MeV·cm). Hence, for a thin target, measuring the energy spectrum of backscattered ions determines both the elements in the target (by measuring E) and the number of atoms for each element (by measuring the number of backscattered ions with energy E).

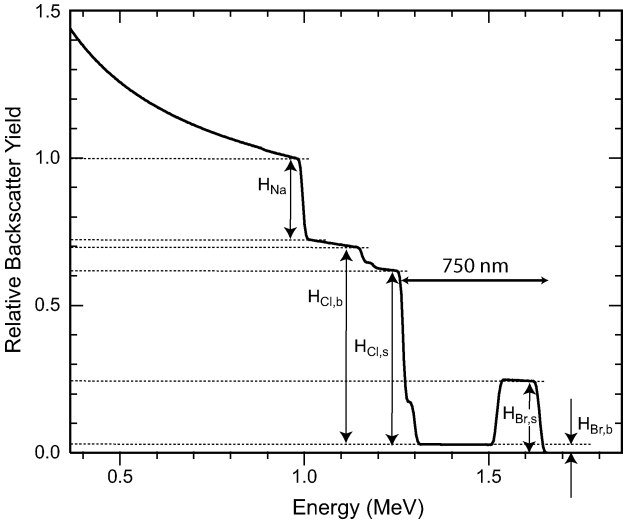

Figure 1. Simulated RBS spectrum of a NaCl−NaBr crystal with a bulk Br/Cl ratio of 0.01 and a 2500 Å thick layer with Br/Cl = 0.1 on the surface. The ordinate is the backscattering yield normalized to the Na surface step height; the abscissa is the energy of the backscattered He^+ ions. The heights H_i of the backscatter signals refers to the target nuclei Br, Cl, and Na and to their position at the surface (s) or in the bulk (b), respectively. The sampling thickness for Br under these conditions is about 750 nm, as indicated by the horizontal arrow. See text for further explanations of how to read the spectrum.

However, in general the samples are thick enough so that the projectile ions lose substantial energy in interactions with the target electrons. In this case, scattering by nuclei residing deeper in the target results in lower backscatter energy than that given by the kinematic factor. The depth of this scattering event can be calculated from the tabulated values of the energy loss factor dE/dx without further calibration. Typically the energy loss factor is expressed as an energy loss per 10^{15} atoms/cm^2, which can be transformed easily into energy loss per depth, if the density of the target material is known. Thus, for thick targets the backscattered energy spectrum is not a series of elemental peaks, but rather a series of elemental steps. The backscatter yield at a specific energy depends on the number of atoms present at a depth corresponding to this energy. Hence, the raw spectrum can be qualitatively read as a concentration profile, with the highest energy giving the surface concentration and lower energies giving concentrations deeper inside the sample.

For this study, data analysis was carried out using the RBS analysis and simulation package RUMP.[25,26]

Example. As an example for the samples of our experiments, a synthetic spectrum of an NaCl−NaBr crystal with a Br enrichment at the surface measured with an incident beam of 2.0 MeV He^+ is shown in Figure 1. The crystal bulk has a homogeneous Br/Cl ratio of 0.01. On top resides a Br-enriched homogeneous 2500 Å thick layer with a Br/Cl ratio of 0.1.

The kinematic factor is highest for Br (0.820) and smaller for the chlorine isotopes ^{37}Cl and ^{35}Cl (0.651 and 0.635, respectively) and Na (0.499), leading to three main steps at 1.640, 1.277 and 0.998 MeV, respectively. The Cl step determines the sampling thickness for Br, because at this and lower backscatter energies, backscattering events from Br atoms are superimposed by backscattering events from Cl atoms leading to a loss in sensitivity for Br. The sampling thickness for Br is calculated from the energy loss of He^+ in the material (see below) to be about 750 nm and indicated in Figure 1. Changes in the backscatter yield within the Br and the Cl steps are reflecting the composition change from the surface layer (at higher energies) to the bulk (at lower energies). The composition of each layer can easily be determined from the individual step heights at the corresponding depth. We will first discuss the surface concentration.

The step height of surface bromine ($H_{Br,s}$) is 0.243 in the relative backscatter yield, and the step height of surface chlorine ($H_{Cl,s}$) is 0.589. The yield ratio $(H_{Br,s})/(H_{Cl,s})$ divided by the Rutherford cross section ratio $(\sigma_{Br}/\sigma_{Cl} = (Z_{Br}/Z_{Cl})^2 = 4.24)$ allows the conclusion that the Br/Cl ratio in the surface layer is 0.1. A similar calculation can be applied to the bulk layer, simply by replacing $H_{Br,s}$ with $H_{Br,b}$ (=0.027) and $H_{Cl,s}$ with $H_{Cl,b}$ (=0.672 relative yield) giving a Br/Cl bulk ratio of 0.01.

The thickness of the surface layer, Δx, can be calculated from the energy loss of the projectile. For NaCl an energy loss factor of 49.95×10^{-15} eV·cm^2 (at 2.0 MeV He^+ incident beam)[46,47] corresponds to an energy loss factor (dE/dx) of 22.3 eV/Å using an atomic density of 4.46×10^{22} atoms/cm^3.[48] The total energy loss, ΔE, is the sum of the energy loss on the inward path (before backscattering) and on the outward path (after backscattering). Hence, the energy loss is related to the thickness of the surface layer by $\Delta E = (dE/dx)\Delta x + K(dE/dx)\Delta x$. Considering the width at half-maximum step height, Br is enriched over a total energy loss of 120 keV, corresponding to an inward and outward path of the He^+ ions through a layer of a thickness of 2957 Å.

The deviation of this estimate from the specified thickness of 2500 Å originates from (1) the neglected contribution of bromine to the density and the energy loss of the target material and (2) the assumption of an energy loss factor constant with depth. This can be accounted for by numerical methods dividing the layer into thin slabs, as done by RUMP,[25,26] replacing the above-mentioned approximations by an accurate physical representation.

The elemental edges are not perfect steps because of the finite energy resolution of RBS experiments. This affects the depth resolution (see section 3.3). Also note that the backscatter yield increases toward lower energy for a homogeneous sample. This is due to the $1/E^2$ dependence in the Rutherford scattering cross section.

Experimental Conditions. RBS experiments were performed on a Dynamitron accelerator in the Ion Beam Laboratory at SUNY-Albany. A beam of $^4He^+$ ions was used with an energy of 2 MeV with typical beam currents of 5 nA. A beam spot area of about 1 mm^2 in diameter was used, thus, all spectra average over this area. This degree of averaging is advantageous, because no heterogeneity of the Br distribution could be observed by SEM (see below) or by moving the beam about the sample in mm-sets. Also, radiation damage can be avoided with such a broad beam. Backscattered ions were counted by a silicon surface barrier detector (energy resolution 15 keV) at a scattering angle of 174° and a solid angle of 4.89 msr. The sample is mounted on a target wheel in high vacuum.

2.2. Sample Preparation. Two types of Br doped NaCl crystals are investigated: first, crystals grown from melt, and second, crystals grown from aqueous solution. The Br/Cl molar ratio of both crystal types is within an order of magnitude of the same range as in seawater, that is, approximately 0.0015. Melt-grown single crystals with a $([Br]/[Cl])_{crst} = 0.01$ were purchased at Korth GmbH, Altenholz, Germany. Crystals from aqueous solution were grown at 293 K from a saturated salt solution by slow evaporation in a Petri dish. The solution was composed of 34.89 g of NaCl, 2.47 g of NaBr, and 100.0 g of H_2O (1.8 wt % NaBr or $([Br]/[Cl])_{sol} = 0.040$). Several crystals nucleated within 1 day and, after about two to 4 days, single crystals of perfect cubic shape with a size of 10 mm × 10 mm × 5 mm were obtained. RBS measurements on cleavage planes of annealed solution-grown crystals give a Br/Cl ratio of 0.002 implying a partition coefficient, p, of 0.05, in good agreement with literature data.[15]

Since Br segregation as a function of exposure to moist air is the main goal of this study, surfaces with an initially uniform and reproducible Br distribution were needed. However, if grown from solution, external surfaces (i.e., those surfaces in contact with the solution during growth)[23,27] as well as (internal) surfaces formed by cleaving the crystal[28] show a strong Br enrichment in the near-surface region compared to the composition of the crystal bulk. Only crystals that have been annealed prior to cleavage provide samples with uniform Br concentrations. Therefore, after removal from the solution, crystals were annealed in a furnace for 3 h at 500 °C surrounded by a constant flow of argon gas. Cleavage planes (001) of such crystals—easily obtained by hammer and chisel—are of good quality except a certain amount of surface steps (see below). Exposure of these crystal surfaces to a defined relative humidity was accomplished by mounting them in enclosed containers over an aqueous solution with appropriate $CaCl_2$ concentration at 293 K.

2.3. Sample Characterization. *Secondary Electron Microscopy (SEM).* Figure 2 shows SEM images taken on cleavage planes of two different annealed solution-grown crystals, not exposed (left panel) and exposed to 65% RH for 130 h (right panel). Note that the cubic shape, corresponding to the crystal habitus of pure NaCl, is well formed in these crystals. No grain boundaries are observed, and the crystals can easily be cleaved parallel to the crystal surfaces. Hence, despite their Br doping, these crystals form large single crystals without apparent grain boundaries. This is in agreement with previous studies on the solid solution of the system NaCl−NaBr,[14−16] where Br^- replaces Cl^- in the NaCl crystal lattice. The hole in the center is a relict of the initial growth stage and is charged with water inclusions and small crystallites. All RBS spectra presented in this study are taken in sufficient distance from the center to be representative for single crystals. No signs of phase separation between NaBr and NaCl or other alterations of the surface structure due to exposure to moist air have been observed with SEM, not even at magnifications 100-times higher than shown in Figure 2.

Atomic Force Microscopy (AFM). AFM experiments (in the tapping mode using the microscope "multimode" from Vecco) were carried out at ambient conditions (room temperature and RH = 30%) to compare the surface morphology of cleavage planes of melt-grown and annealed solution-grown crystals. Several surface scans with a horizontal resolution of 20 nm or better were made. One typical example for each type is shown in the left panel of Figure 3 along with the corresponding morphological profiles in the right panel. No AFM surface scan

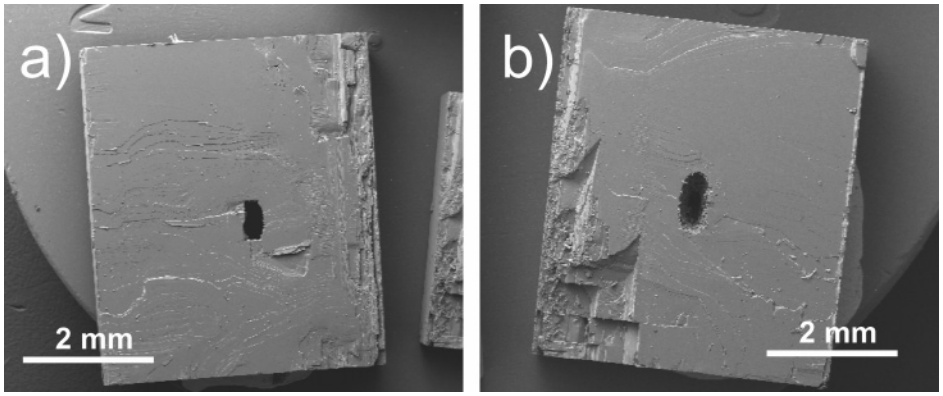

Figure 2. SEM images (BSE mode) of cleavage planes of annealed solution-grown crystals with a Br/Cl bulk ratio of 0.002. The left panel shows a crystal plane not exposed to humidity, the right panel shows a crystal plane after exposure to 65% RH for 130 h.

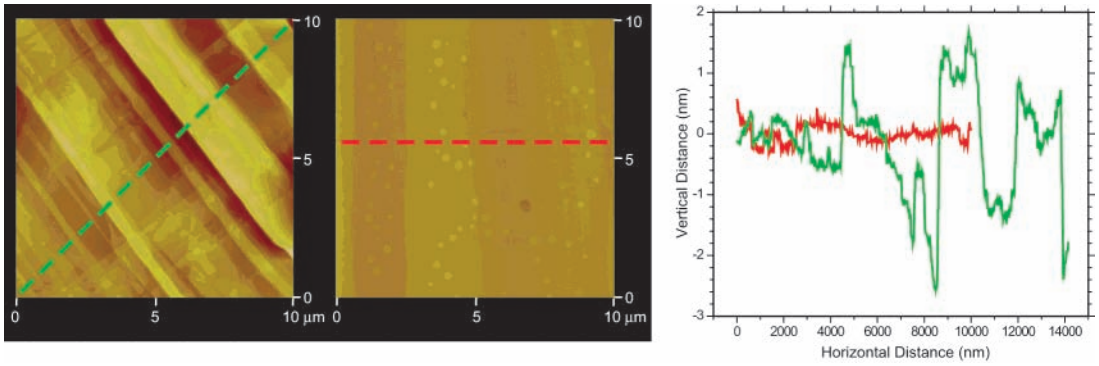

Figure 3. Typical surface topography of a cleavage plane of an annealed crystal grown from aqueous solution (left picture, left panel) and from melt (right picture, left panel), as measured by AFM. Corresponding profiles along the indicated lines are shown in the right panel.

showed inhomogeneities like pores, crystallites, or other signs of phase separation. The only identified defects are surface steps. The surfaces of crystals grown from melt (right picture, red profile) are almost perfectly flat except for very few surface steps with a height in the order of one atomic layer. An example is the darker appearing trench with a depth of about 3 Å (1 layer) and a width of about 2 μm on the left side in the picture. The small white spots with a circlelike outline are small elevations by a few Å. They did not move during measurement and did not occur on all examined samples implying that they are relicts of the crystal cleavage. The surface roughness is increased by a factor of 5 to 10 on cleavage planes of solution-grown crystals (left picture, green profile). One explanation for the difference in the surface-step height is that crystals from solution, despite annealing, exhibit more irregularities in the lattice leading to less perfect cleavage planes (notwithstanding their single crystalline nature).

3. Results

3.1. RBS on NaCl−NaBr Crystals Exposed to Different Relative Humidities. Using RBS, Br-concentration profiles in the near-surface region (i.e., ∼100 nm) of Br-doped NaCl crystals grown from melt and of annealed crystals grown from aqueous solution were measured after exposure to 20%, 50%, and 65% RH. These humidities were chosen for the following reason: 20% RH is well below the humidity at which multilayer water adsorption on NaCl surfaces occurs, whereas 50% and 65% RH are both within the multilayer adsorption regime.[30] A value of 50% RH is lower and 65% RH is higher than the deliquescence relative humidity (DRH) of NaBr (58%), but both are still well below the DRH of NaCl (75%).[6]

The results are outlined in Figure 4 for solution-grown crystals with Br/Cl = 0.002 exposed to 20%, 50%, and 65% RH and for melt-grown crystals with Br/Cl = 0.01 exposed to 65% RH. Each left panel shows the number of segregated Br atoms as a function of exposure time. Black data points mark measurements on single samples with error bars derived from counting statistics. All crystals were only measured once, thus, each data point refers to a cleavage plane of a different crystal. The scatter in data points of the left panels in Figure 4 is large and cannot be explained by counting statistics alone. Only the unexposed samples and samples exposed to 20% RH show scatter consistent with counting statistics. As statistical error and scatter between samples are high, spectra, which were taken between certain time intervals, are averaged and plotted as filled colored squares. With the use of the same color scheme, the corresponding averaged spectra are shown in the right panels. For comparison, they are overlaid with a simulated RBS-spectrum assuming homogeneous bulk composition (black solid line). The Br surface enrichment can be seen in the spectra between 1.60 and 1.65 MeV, which corresponds to the energy of ions scattered from Br atoms just at the surface. While the thickness of the Br enriched surface layer cannot be resolved in our measurements (see section 3.3), the integrated amount of Br segregation into this layer (i.e., extra surface Br atoms cm^{-2}) is reliably determined from the counts in the surface peak.

Annealed Solution-Grown Crystals. In annealed crystals grown from solution, the surface can be enriched in Br depending on humidity and exposure time. At 20% RH (Figure 4a), the spectra show a constant Br profile and no surface Br layer develops even after about 1000 h of exposure. In contrast, on crystals exposed to 50% and 65% RH (Figure 4b,c) substantial surface segregation of Br occurs until a saturation level is reached. On the basis of the red data point, saturation levels with $(0.24 \pm 0.11) \times 10^{15}$ Br atoms cm^{-2} at 50% RH and $(0.42 \pm 0.12) \times 10^{15}$ Br atoms cm^{-2} at 65% RH are

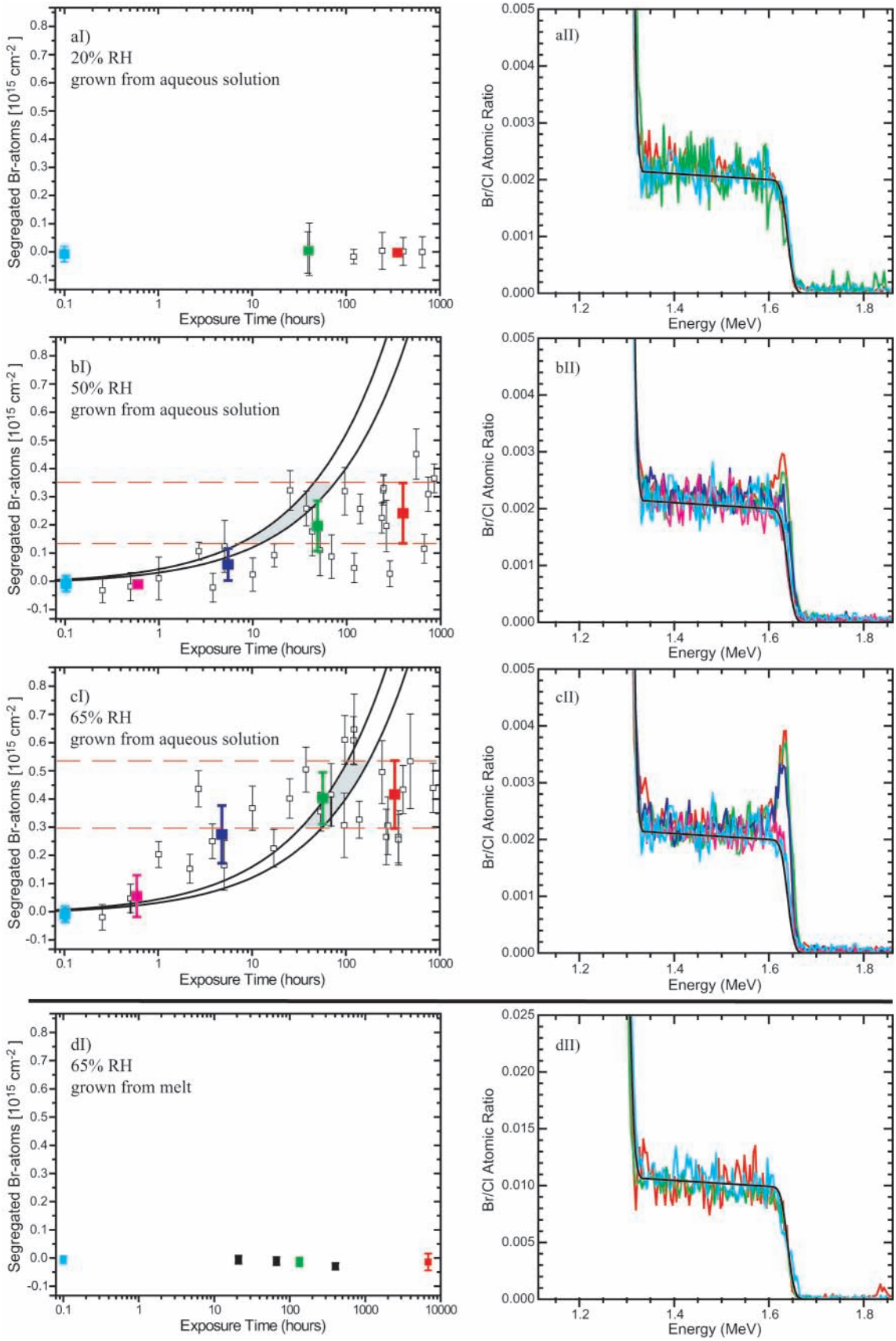

Figure 4. Left column (I) shows Br segregation of annealed solution-grown crystals (Br/Cl = 0.002) exposed to (a) 20%, (b) 50%, and (c) 65% RH and of (d) melt-grown crystals (Br/Cl = 0.01) exposed to 65% RH. Solid lines represent maximum segregation given by bulk diffusion of Br in NaCl. Dashed red lines represent observed saturation level. Open squares represent segregated Br atoms per area measured on single samples with error bars representing the error from counting statistics. Filled colored squares are averaged data for certain time regions ($t = 0$ h, 0 h $< t \leq 1$ h, 1 h $< t \leq 10$ h, 10 h $< t \leq 100$ h, 100 h $< t \leq 1000$ h, 1000 h $< t$) with error bars representing the standard deviation from the mean value. Right column (II) shows spectra corresponding to the averaged data (colored points in left panel). In addition, a simulation assuming homogeneous bulk composition is overlaid as a thin black line.

observed and marked in the corresponding plots by the red dashed lines. As solid-state diffusion is one candidate process for the transport to the salt surface, we compare the observed kinetics with a diffusive kinetics. The solid lines in the left panels indicate the maximum segregated Br atoms given by solid-state diffusion of Br in NaCl (Appendix A), which was measured on an annealed solution-grown crystal under dry conditions. The grayish field corresponds to the zone where a purely diffusion-limited segregation would reach the saturation zone and stop. A *t*-test of data points between the center of the grayish field and 1000 h shows that there is no significant slope at both humidities (*p*-values are 0.13 for the 50% RH data and 0.60 for the 65% RH data). Together with the fact that at exposure times beyond the grayish field, solid-state diffusion would allow much more Br segregation than observed at both humidities, this enforces the conclusion that Br segregation reaches a saturation level.

Solid-state diffusion seems to set an upper limit for the segregation of Br atoms to the surface at 50% RH implying that at this humidity, kinetics is controlled by solid-state diffusion. However, if the humidity is enhanced to 65% RH, segregation in the initial phase, for example, for data points with $t < 100$ h at 65% RH, is faster than consistent with solid-state diffusion. This implies an additional effect at this higher humidity accelerating the segregation of Br, for example humidity-driven partial dissolution of the surface or the formation of liquidified shortcuts in the salt crystal.

Melt-Grown Crystals. Six experiments at different exposure times have been performed on crystals grown from melt exposed to 65% RH (Figure 4d). The light-blue spectrum marks the zero measurement on a crystal not exposed to humidity, the green and the red spectra mark the measurement after about 6 and 285 days, respectively (Figure 4dII). Even after 285 days, no surface peak develops and the calculated Br segregation is consistent with zero (Figure 4dI).

3.2. RBS Measurements on Scratched Cleavage Planes of Melt-Grown Crystals. To evaluate the effect of the surface structure on Br segregation, a cleaved surface from a melt-grown crystal was roughened with a diamond scraper prior to exposure. The result is shown in Figure 5. A photograph of the crystal surface is shown in the top panel. An area of about 5 mm × 5 mm in the central part appears darker because of roughening. The dark spots with an area of about 1 mm^2 are beam induced color centers and indicate the location where the beam has hit the target. The gray arrow points to the location where the RBS spectrum (gray line in the bottom panel) is taken immediately after scratching.[29] Such a roughened surface was then exposed for 404 h to 65% RH. The black line in the bottom panel is the sum of the spectra taken at the three locations indicated by the black arrows in the top panel. A distinct surface peak developed in the scratched region after exposure to humidity. In contrast, no segregation occurs in the unscratched regions at the top and bottom left corners of the crystal (spectra not shown). The experiment was repeated twice for different exposure times (4 d, 220 d) leading to a comparable size of the surface peak. Hence, on cleavage planes of crystals grown from melt, only where the surface was roughened prior to exposure to humidity is Br surface segregation observed.

3.3. Depth Resolution of the RBS Experiment. The width of the Br surface peak in the experiments shown in Figure 4 is generally in the range of 25 to 35 keV, whereas the expected energy resolution of the silicon RBS detector is about 15 keV. This naturally raises the question: does the 25−35 keV width of Br surface peak indicate a significant depth distribution of the Br or is this width due to some other experimental limitation? A possible source of increased detector energy resolution beyond the expected 15 keV is the possible electrical charging of the salt targets by the 2 MeV He^+ beam. To check this possibility, RBS measurements were repeated under conditions that should reduce the electrical charging. Namely, the beam current was reduced to ∼3 na, the beam spot was enlarged, and an electron-emitting filament was installed next to the target.

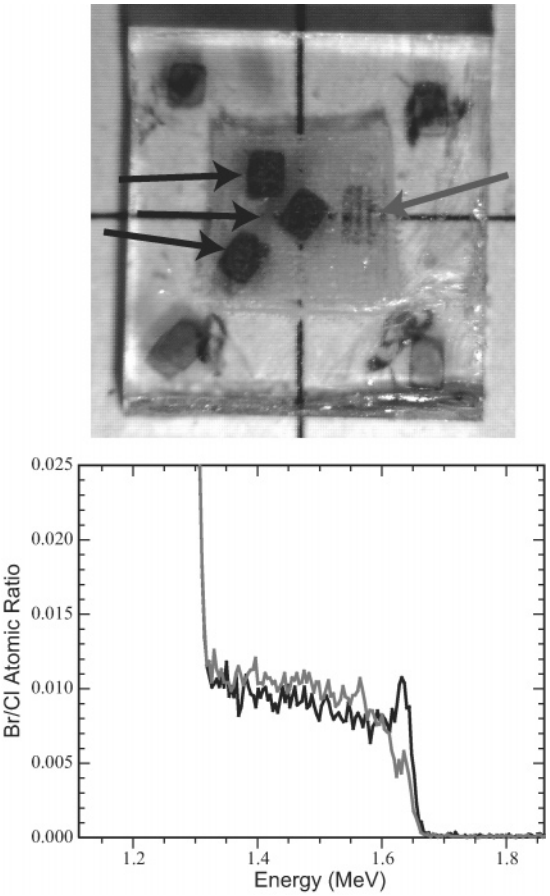

Figure 5. Upper panel is a photograph of a crystal grown from melt (Br/Cl = 0.01) with an artificially roughened surface in the central part. The dimension of the crystal is 1 cm × 1 cm. It was measured before (gray arrow) and after exposing to 65% RH for 404 h (black arrows). The dark squares are the locations where the beam has hit the target. Lower panel shows the corresponding spectra before exposure (gray line) and after exposure (black line).

A spectrum recorded under the special conditions described above on a sample exposed to 65% RH for 2350 h (thick solid line) is shown in Figure 6 along with a simulation assuming 0.4×10^{15} Br atoms cm^{-2} on the surface of the crystal (thin solid line). The width at half-maximum for the Br surface peak is now 18 keV, corresponding to a layer thickness of 44 nm (see example in section 2.1). Thus, improving the depth resolution of the experiment leads to a reduction of the energy width of the Br surface peak from 25 to 35 to ∼18 keV. Hence, it is clear that the width of the Br surface peak is limited by the experimental depth resolution of this RBS setup, and 44 nm represents an upper limit of the thickness of the Br enriched surface layer. Therefore, all RBS simulations used here assumed very thin surface layers. We did not make all measurements under these special running conditions because they significantly increased the run times (both because of the reduced beam current and because of the time needed to carefully adjust the filament current).

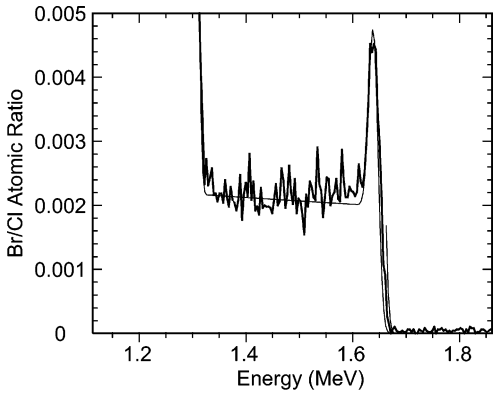

Figure 6. RBS on a cleavage plane of an annealed solution-grown crystal exposed to 65% RH for 2350 h. Abscissa is the energy of the backscattered He^+ ions; ordinate is the absolute backscatter yield. The thick solid line represents RBS spectra taken under optimized technical conditions to achieve the best possible energy resolution (~18 keV). Thin solid line is a simulation assuming a segregation layer of 0.4×10^{15} Br atoms cm^{-2}.

It is important to emphasize that RBS reliably gives the Br enrichments in atoms/cm^2 within the depth resolution of the method and independent of the filament current.

4. Discussion

Below we will outline a possible mechanism leading to the Br surface segregation reported here. However, before doing this, let us summarize the key experimental observations:

(1) No Br surface segregation is observed on cleaved surfaces of crystals grown from melt, even after very long exposure to 65% relative humidity.

(2) Contrary to the results for melt-grown crystals, Br surface segregation is observed on cleaved crystals grown from solution, with Br enrichment increasing with exposure time and with relative humidity. The thickness of the Br-enriched layer is less than the depth resolution of RBS (~44 nm). Hence, only the amount of extra surface Br in atoms/cm^2 is determined by RBS.

(3) The two observations listed above suggest that crystal surface defects (including impurities) play an essential role in the mechanism leading to surface segregation. Other evidence for this conclusion is the observation of Br-surface enrichment on melt-grown crystals exposed to moist air subject to prior surface abrasion.

In the following, we will show that these experimental observations can be explained as the result of the Br partitioning between the solid crystalline bulk and an adsorbed liquid layer on the surface.

Water adsorption on well-defined surfaces of melt-grown NaCl crystals has been intensively studied.[30] The coverage increases with increasing water vapor pressure and evolves from submonolayer to multilayer coverage (i.e., from liquid island formation with 2-D growth to full cover 3-D growth) at room temperature at about 40% RH.[33−35] At 50% RH a coverage of ~3 adsorption layers is expected, and at 65% RH about 3.5 is expected.[33] This goes along with a 3-D growth of a water-molecule network. Above a critical RH of about 40%, ions will dissolve into this adsorption layer. The presence of such a layer has been implied by a jump in surface conductivity at approximately 50% RH owing to dissolved ions as charge carriers,[36] by surface step mobility above 40% RH on NaCl crystals[37−39] and by IR spectroscopy.[33,34] There is no stable bulk solution below the DRH of NaCl (75%[6]). Such an adsorbed liquid layer is stable only because its chemical potential is lowered with respect to a bulk solution of the same composition by a surface energy term, similar to what has been observed on solids approaching the bulk melting temperature (e.g., ref 40). This surface energy term is determined by surface forces stabilizing the adsorbate, in this case adsorbed water with Na^+, Cl^-, and Br^- ions mixed into it. Moreover, it is influenced by the local curvature of the surface (Kelvin effect).[41] The ion concentration of this layer is not exactly known but assumed to correspond with the one of a saturated salt solution although values by a factor of 2 higher or lower are conceivable.

In thermodynamic equilibrium, Br concentration in the adsorbed liquid layer will be enhanced compared to bulk because of the partitioning of Br between the adsorbate and the crystal. In the absence of any better value, we will assume a coefficient, p_{layer}, of similar magnitude than for partitioning between liquid and solid solution, that is, $p_{layer} \approx p = ([Br]/[Cl])_{crst}/([Br]/[Cl])_{sol}$. In literature, values of p range from 0.014 to 0.045, with the lowest values corresponding to measurements on very slowly grown crystals or calculations for thermodynamical equilibrium.[14,15,18−21] Crystals used in our study were grown relatively fast (2 to 4 days) and a partition coefficient of 0.050 was measured with RBS. Hence, based on the assumption that ions from the bulk are incorporated into the adsorbed liquid layer according to a partition coefficient between 0.014 and 0.050, the Br/Cl ratio on the surface is enhanced by a factor between 20 and 70 ($= 1/p$) compared to the crystal bulk.

The RBS technique cannot directly measure the thickness of the adsorbed liquid layer because of drying during evacuation of the measurement chamber. If one assumes bulk concentration in this layer, the evaporation of water leads to a thinning of the layer by about a factor of 5. The experiment with the improved depth resolution shown in section 3.3 has allowed a determination of an upper limit of the Br enriched layer of the dried crystal of 44 nm, or ~220 nm of the adsorbed liquid layer. This value is consistent with our data. Even a monolayer of Br on top of the solid bulk would result in the experimentally observed spectra.

However, the total number of excess Br atoms in the surface layer is determined accurately by RBS. Therefore, it is possible to estimate the thickness of the adsorbed liquid layer from the measured Br concentration on the surface if one assumes that $0.014 \leq p_{layer} \leq 0.050$ and that the salt concentration in the adsorbed liquid layer does not differ by more than a factor of 2 from a saturated salt solution. For example, at 65% RH at saturation (red data point in Figure 4aI, $t \approx 50$ h) 0.42×10^{15} Br atoms cm^{-2} have dissolved into this layer implying a thickness between 7 and 59 nm. The same calculation for 50% RH yields a thickness between 4 and 34 nm. Because of the long time scales of our experiments, we believe that thermodynamic equilibrium is approached and that a low partition coefficient of about 0.014 is a reasonable assumption leading to thicknesses of the adsorbed liquid layer between 4 and 7 nm, depending on relative humidity. This is comparable with the water adsorption measured on a single levitated micronscale aerosol particle with the same composition as in the experiments described here.[42]

As shown in a previous work,[37] exposure to moist air leads to smoothing rather than roughening of the NaCl crystal surface. Specifically, the assumption that recrystallization of NaBr on top of the NaCl−NaBr crystals drives the surface segregation can be excluded on the basis of the absence of NaBr crystallites in the AFM and SEM images presented here. Hence, we conclude that segregation must occur in a thin layer on top of the crystal. This argument is further corroborated by the fact

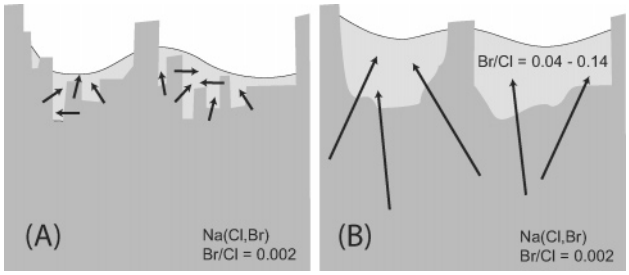

Figure 7. Sketch of the "2-stage-model" for Br surface segregation owing to exposure to moist air. (A) Multilayer water adsorption and incorporation of ions located at surface defects leading to partial annealing of the surface. Dissolution of ions causes further water adsorption and formation of an adsorbed liquid layer. (B) Diffusion limited incorporation of ions into this layer from larger depth until Br/Cl ratio satisfies the partition coefficient. Given that $0.014 \leq p \leq 0.050$, the Br/Cl ratio in the adsorbed liquid layer is enhanced by a factor between 20 and 70.

that a recrystallization process is thermodynamically not favored. At room temperature, NaBr−NaCl crystals form solid solutions[14−16] and NaBr crystals are not expected to form. Physical properties of crystals with a composition as in our experiments are close to those of pure NaCl. This also holds for the deliquescence, which occurs at RH close to the one of pure NaCl. The presence of a solid solution is in agreement with the finding that Br segregation occurs above and below the DRH of pure NaBr (58%) to a comparable degree.

While the adsorption of water should be a fast process, the observed Br segregation takes many hours. Therefore, we propose a two-stage process (Figure 7): (A) An adsorption layer forms that partly dissolves and anneals the crystal surface and incorporates ions at molar ratios reflecting the crystal's surface composition. (B) Br moves to the adsorbed liquid layer to satisfy Br partitioning between solid and liquid.

The kinetics of this movement is limited by solid-state diffusion of the Br^- ions through the crystalline matrix. The time to reach equilibrium for the Br concentration in the surface layer is about consistent with the characteristic time of Br diffusion in NaCl. According to this model, the partition coefficient determines the enhancement of the Br/Cl ratio on the surface, while the thickness of the adsorbed liquid layer determines the total number of segregated Br atoms per unit area. This model can explain the slow Br segregation during the first hours of exposure (formation of the adsorbed liquid layer) and the saturation reached afterward (adjustment of the partition coefficient) as well as the humidity dependence of the surface enrichment (thickness of the adsorbed liquid layer is given by the relative humidity).

It was also shown in Figure 4 that no Br segregation was detected in crystals grown from melt, not even after 1 year of exposure to moist air. Applying the same calculation from above and assuming a detection limit[24] of 0.1×10^{15} Br atoms cm^{-2} one can estimate the upper limit of the thickness of the adsorbed liquid layer in these crystals to be between 0.5 and 3.1 nm, which is in good agreement with thicknesses determined in previous studies on melt-grown NaCl crystals.[33,34] Hence, Br segregation in melt-grown crystals might exist, but the volume of adsorbed water is too small to provide a sink big enough for a Br enrichment detectable with RBS. Using X-ray photoelectron spectroscopy (XPS), Ghosal et al.[22] measured a surface enrichment by a factor of more than 10 of bromine in Br-doped melt crystals (bulk composition Br/Cl = 0.07) after exposure to 54% RH for several hours. This is not in contradiction to our results. XPS is sensitive to the top few atomic layers of the crystal, while the surface peak in the RBS spectra is an average over the upper 44 nm. In addition, the higher bromine bulk concentrations might enhance Br-surface enrichment: according to our model, Br segregation is directly proportional to $([Br]/[Cl])_{crst}$ with p as the constant of proportionality. Also, phase separation between NaCl and NaBr was observed by SEM,[22] which might influence Br segregation.

The reason the thickness of the adsorbed liquid layer is so much larger in solution-grown crystals than in melt-grown ones remains speculative. The difference cannot be explained by differences in solid-state diffusion for melt- and solution-grown crystals since this process is similarly fast for both crystal types (Appendix A) and occurs fast enough to lead to a visible Br segregation in the timescales of the experiment (Figure 4). However, there are indications that the difference originates in the surface properties. First, crystals grown from melt only show Br segregation, if the surface is artificially roughened prior to exposure (Figure 5). Second, the scatter of single data points in Figure 4b and c is not determined by the measurement precision and can only be explained by structural differences. Third, AFM shows that surface steps in cleavage planes of solution-grown crystals are higher and more frequent than in melt-grown crystals (Figure 3). Some of these surface defects might favor water adsorption as has been previously observed on defect-rich NaCl surfaces (e.g., refs 43 and 44). In addition, it has been found that dissolution is influenced strongly by surface defects (e.g., ref 45). However, a quantitative relation between surface structure and water adsorption of our crystals is not feasible with the experimental evidence at hand. Nevertheless, the presented results show clear evidence that a multilayer H_2O adsorption is necessary to initiate substantial Br-surface enrichment and that bromine segregates to this adsorbed liquid layer because of its higher aqueous solubility compared with Cl.

5. Atmospheric Implications

Most sea-salt aerosols in the natural environment are liquid, because they remain in the marine boundary layer, where the relative humidity is typically around 80%. Thus, solution microphysics and chemistry will determine the distribution of halogens in the aerosol and in the ambient air. Efflorescence of NaCl as the main component of sea-salt aerosols occurs at about 40% RH. Hence, partial crystallization of sea-salt aerosols occurs only if they are formed in regions where the relative humidity is sufficiently low (e.g., in salt deserts or in freeze-dried polar regions[49]), or if they are transported over large distances into drier regions (e.g., refs 3 and 4). Sea-salt aerosols under realistic atmospheric conditions will not completely crystallize, because they contain a large fraction of hygroscopic Mg- and K-salts, such as $MgCl_2$, $MgSO_4$, and $KMgCl_3$, which remain liquid even under driest conditions present in the troposphere. For instance, according to Tang et al.,[50] about 25% by mass of the sea-salt particle is liquid at 40% RH and about 15% at 10% RH. The shape of effloresced salt particles depends mainly on the rate of evaporation and on the nature of the solute. A variety of shapes have been found for dried sea-salt particles. For instance, Weis and Ewing[51] found anomalously high water content in NaCl crystals effloresced from 0.1-μm-sized droplets and concluded that such particles contain pores and pockets filled with aqueous NaCl solution even well below the NaCl efflorescence relative humidity. Theoretical considerations show that compounds without a strong crystal habit (like sea salt) are likely to form cenospheres with relatively smooth, solid surfaces rather than single or polycrystals.[52] The formation of

a solid shell on a liquid droplet during efflorescence (eventually collapsing) has also been observed experimentally.[53] The resulting particle shapes are hollowed spherical shells, sometimes containing holes from crystal growth.

In addition, low temperatures could also lead to the formation of solid sea-salt particles. Namely, if the temperature drops below ca. 233 K,[54] ice may precipitate and trigger salt crystallization. This mixed ice/salt particle will remain solid up to the eutectic temperature of 238 K.

In summary, there is evidence for regions sufficiently dry or cold for NaCl to crystallize and to be exposed to the gas phase. This NaCl crystal will incorporate a certain amount of bromine, and partitioning of Br between the solid and the liquid phase occurs. In principle, the final equilibrium distribution of Br between the phases is determined by the partition coefficient with the Br concentration in the liquid phase being enhanced. However, since the absolute amount of Br is limited, this can only be achieved in particles with high solid-to-liquid volume ratios. Hence, we believe that Br partitioning is most efficient between NaCl crystallized as a solid shell of the particle and a thin, adsorbed water film on the surface of the crystal. The Br enrichment in this layer can be estimated as follows: According to partition coefficients measured in our and other studies in the system NaCl−NaBr, the Br/Cl ratio in the liquid is enhanced by a factor of 20−70 compared to the solid (for p between 0.014 and 0.050). The partition coefficient for Br in NaCl is decreased by a factor of about 2, if Mg^{++} ions in a concentration similar to that in seawater are present.[17] This leads to a Br enrichment in the liquid of mixed phase sea-salt aerosols by a factor of 40 to 140 or a Br/Cl molar ratio of up to 0.2 compared to 0.0015 in seawater.

Partitioning was found to be almost independent of the Br/Cl molar ratio at low Br concentrations.[15] Therefore, we assume that the difference in the Br concentration between our experiments and natural sea salt does not lead to misinterpretations concerning atmospheric implications. The effect of the temperature is small. Increasing the temperature from 25 to 83 °C enhances the partition coefficient of Br in crystallized sea salt by less than 10%.[15] In our experiments on single crystals we found that solid-state diffusion is limiting the transport of bromine into the liquid. In nature, solid sea-salt aerosols are mainly polycrystalline with pores, veins, grain boundaries, fractures, and other discontinuities, which provide a diffusion pathway fast enough to allow very rapid partitioning.

As mentioned previously, partitioning will be most effective if the particles show high solid-to-liquid volume ratios, which may be the case in a cold and dry environment. Of course, under these conditions, freezing and precipitation of ice, hydrates, and other complex compounds may have additional unknown impact on bromine partitioning.

These considerations show that the bromine concentration in the liquid phase or in adsorbed surface water of mainly crystallized sea-salt aerosols might be enhanced by a factor of up to 140. This implies that solid aerosols can act as a bromine source for the gas-phase even more efficiently than liquid droplets.

Acknowledgment. We gratefully thank Art Haberl and Wayne Skala from the Ion Beam Laboratory, SUNY at Albany, for the excellent support concerning all questions around the SUNY particle accelerator. We also thank Roland Brütsch (PSI) for the electron microscopy measurements and Rolf Schelldorfer (PSI) for performing the AFM analysis. We are also grateful to Atsumu Ohmura, Peter Spichtinger, and Andrew Gettelman who have provided helpful discussions. Finally, we would like to acknowledge our discussions with Beiping Luo and Joerg Maeder and also Uwe Weers and Edwin Hausammann for all the technical support. This research has been funded by the ETH Zurich under Grant TH-2202-2.

Appendix

A. Calculation of Maximum Surface Segregation by Solid-State Diffusion. The maximum surface segregation given by solid-state diffusion was determined by mounting a Br-doped NaCl crystal (Br source) onto a pure NaCl crystal (Br sink) and measuring the Br concentration profile with RBS on the contact surfaces after a certain time.[32] Fitting the resulting profile to an error function[31] yields a diffusion constant at 20 °C of $D = (2.3 \pm 0.5) \times 10^{-16}$ cm^2 s^{-1} for melt-grown crystals and $D = (1.3 \pm 0.4) \times 10^{-16}$ cm^2 s^{-1} for annealed solution-grown crystals. Diffusion constants for melt-grown and annealed solution-grown crystals are found to be about the same at any temperature measured from 20 to 600 °C, while the absolute value changes by 5 orders of magnitude. If the kinetics of Br segregation was limited by solid-state diffusion, the characteristic thickness of the Br enriched layer can be estimated using $\langle x \rangle = \sqrt{Dt}$. Atomic density of Br in the bulk is $\rho_{Br} = 0.45 \times 10^{20}$ cm^{-3} for the solution-grown and $\rho_{Br} = 2.21 \times 10^{20}$ cm^{-3} for the melt-grown crystals. Thus, the maximum area number density of segregated Br atoms is $Br_{layer} = \rho_{Br}\langle x \rangle = k\sqrt{t}$, with $k = \rho_{Br}\sqrt{D} = (5.1 \pm 0.7) \times 10^{11}$ cm^{-2} s$^{-1/2}$ for solution-grown crystals and $k = (33.6 \pm 4.0) \times 10^{11}$ cm^{-2} s$^{-1/2}$ for melt-grown crystals. This function describes a situation where Br surface segregation is completely controlled by solid-state diffusion and is framed by the solid lines in the left panels of Figure 4b,c for solution-grown crystals.

References and Notes

(1) Andreae, M. O. In *World Survey of Climatology*; Henderson-Sellers, A., Ed.; Elsevier: Amsterdam, The Netherlands, 1995; Vol. 16, p 341.
(2) Finlayson-Pitts, B. J. *Chem. Rev.* **2003**, *103*, 4801.
(3) Shaw, G. E. *J. Geophys. Res.* **1991**, *96*, 22369.
(4) Ikegami, M.; Okada, K.; Zaizen, Y.; Makino, Y. *Tellus* **1994**, *46B*, 142.
(5) Woods, D. C.; Chuna, R. L.; Rose, W. I. *Science* **1985**, *230*, 170.
(6) Martin, S. T. *Chem. Rev.* **2000**, *100*, 3403.
(7) Junge, C. E. *Tellus* **1956**, *8*, 127.
(8) Finlayson-Pitts, B. J.; Hemminger, J. C. *J. Phys. Chem. A* **2000**, *104*, 11463.
(9) Barrie, L. A.; Bottenheim, J. W.; Schnell, R. C.; Crutzen, P. J.; Rasmussen, R. A. *Nature* **1988**, *334*, 138.
(10) Platt, U.; Hönninger, G. *Chemosphere* **2003**, *52*, 325.
(11) Hebestreit, K.; Stutz, J.; Rozen, D.; Matveiv, V.; Peleg, M.; Luria, M.; Platt, U. *Science* **1999**, *283*, 55.
(12) Vogt, R.; Crutzen, P. J.; Sander, R. *Nature* **1996**, *383*, 327.
(13) Sander, R.; Keene, W. C.; Pszenny, A. A. P.; Arimoto, R.; Ayers, G. P.; Baboukas, E.; Cainey, J. M.; Crutzen, P. J.; Duce, R. A.; Hönninger, G.; Huebert, B. J.; Maenhaut, W.; Mihalopoulos, N.; Turekian, V. C.; Van Dingenen, R. *Atmos. Chem. Phys.* **2003**, *3*, 1301.
(14) Boeke, H. E. *Z. Kristallogr. Mineral.* **1908**, *45*, 346.
(15) Braitsch, O.; Herrmann, A. G. *Geochim. Cosmochim. Acta* **1963**, *27*, 361.
(16) Pies, W.; Weiss, A. Solid solutions of simple bromines with hydrides, fluorides, and chlorides. In *Landolt-Börnstein: Group III Condensed Matter;* Springer-Verlag: New York, 1973; Vol. 7/1, p 572.
(17) Herrmann, A. G. *Chem. Geol.* **1980**, *28*, 171.
(18) Puchelt, H.; Lutz, F.; Schock, H. H. *Naturwissenschaften* **1972**, *59*, 34.
(19) Lutz, F. Dissertation, Eberhard-Karls-Universität, Tübingen, Germany, 1975.
(20) Siemann, M. G.; Schramm, M. *Geochim. Cosmochim. Acta* **2000**, *64*, 1681.
(21) Stoessell, R. K.; Carpenter, A. B. *Geochim. Cosmochim. Acta* **1986**, *50*, 1465.
(22) Ghosal, S.; Shbeeb, A.; Hemminger, J. C. *Geophys. Res. Lett.* **2000**, *27*, 1879.

(23) Zangmeister, C. D.; Turner, J. A.; Pemberton, J. E. *Geophys. Res. Lett.* **2001**, *28*, 995.
(24) Chu, W. K.; Mayer, J. W.; Nicolet, M. A. *Backscattering Spectrometry*, Academic Press: New York, 1978.
(25) Computer Graphic Service. *RUMP*, version 4.00 (beta); http://www.genplot.com (accessed 2004).
(26) Doolittle, L. R. *Nucl. Instrum. Methods Phys. Res.* **1985**, *9B*, 344.
(27) The aqueous solution the crystal is exposed to during growth has a higher Br concentration. After removal from the solution, we dried crystals first by a tissue, then by air, and finally by evacuating in the analyzing chamber. Nevertheless, a considerable amount of Br-enriched crystallites was left on the surface. This was experimentally not controllable, and we observed large fluctuations in the amount of extra Br on the surface, with an average value of about 9.7×10^{14} Br atoms/cm^2. This corresponds to an enrichment by 290% on the top 130 nm, compared to bulk concentration.
(28) NaCl−NaBr crystals exhibit a large amount of micropores after crystal growth. These pores are filled with a Br-enriched aqueous solution. Cleavage through these pores results in a release and a draining of the pore water onto the newly formed surface. This cleavage induced Br segregation exceeds 1 μm depth. While this enrichment is large and reproducible, there are large fluctuations in the amount of Br enrichment observed.
(29) This spectrum apparently shows a depletion of Br on the surface, which is also observed for Cl. Therefore, this is not attributed to a chemical alteration, but rather to an artifact from surface roughness or channeling, which are known to affect the yield of backscattered ions under certain circumstances.[24]
(30) Ewing, G. E. *J. Phys. Chem. B* **2004**, *108*, 15953.
(31) Carslaw, H. S.; Jaeger, J. C. *Conduction of Heat in Solids*; Clarendon Press: Oxford, U.K, 1959.
(32) Hess, M.; Krieger, U. K.; Lanford, W. A. Manuscript in preparation.
(33) Foster, M.; Ewing, G. E. *Surf. Sci.* **1999**, *427*−*428*, 102.
(34) Foster, M.; Ewing, G. E. *J. Chem. Phys.* **2000**, *112*, 6817.
(35) Engkvist, O.; Stone, A. J. *J. Chem. Phys.* **2000**, *112*, 6827.
(36) Hücher, M.; Oberlin, A.; Hocart, R. *Bull. Soc. Fr. Mineral. Cristallogr.* **1967**, *90*, 320.
(37) Dai, Q.; Hu, J.; Salmeron, M. *J. Phys. Chem. B* **1997**, *101*, 1994.
(38) Shindo, H.; Ohaski, M.; Baba, K.; Seo, A. *Surf. Sci.* **1996**, *111*, 357.
(39) Shindo, H.; Ohaski, M.; Tateishi, O.; Seo, A. *J. Chem. Soc., Faraday Trans.* **1997**, *93*, 1169.
(40) Wettlaufer, J. S.; Grae, Worster, M. *Annu. Rev. Fluid Mech.* **2006**, *38*, 427.
(41) Thomson, S. W. *Philos. Mag.* **1871**, *4*, 448.
(42) Krieger, U. K.; Gasser, L.; Marcolli, C.; Huthwelker, T.; Peter, T. Manuscript in preparation.
(43) Dai, D. J.; Peters, S. J.; Ewing, G. E. *J. Phys. Chem.* **1995**, *99*, 10299.
(44) Ewing, G. E.; Peters, S. J. *Surf. Rev. Lett.* **1997**, *4*, 757.
(45) Lasaga, A. C.; Luttge, A. *Eur. J. Miner.* **2003**, *15*, 603.
(46) Particle Interactions with Matter. http://www.srim.org (accessed 2006).
(47) Ziegler, J. F.; Biersack, J. P.; Littmark, U. *The Stopping and Range of Ions in Solids*; Pergamon Press: New York, 1985; Vol. 1.
(48) Lide D. R. *CRC Handbook of Chemistry and Physics*; CRC Press: Boca Raton, FL, 1998−1999.
(49) Gettelman, A.; Walden, V. P.; Miloshevich, L. M.; Roth, W. L.; Halter, B. *J. Geophys. Res.* **2006**, *111*.
(50) Tang, I. N.; Tridico, A. C.; Fung, K. H. *J. Geophys. Res.* **1997**, *102*.
(51) Weis, D. D.; Ewing, G. E. *J. Geophys. Res., D* **1999**, *104*, 21275.
(52) Leong, K. H. *J. Aerosol Sci.* **1987**, *18*, 511.
(53) Braun, C.; Krieger, U. K. *Opt. Express* **2001**, *8*, 314.
(54) Koop, T.; Kapilashrami, A.; Molina, L. T.; Molina, M. J. *J. Geophys. Res.* **2000**, *105*, 26393.